4-oxo-2-nonenal-induced α-synuclein oligomers interact with membranes in the cell, leading to mitochondrial fragmentation

Andersen, Camilla; Lausdahl, Astrid K. ; Nielsen, Janni; Clausen, Mathias Porsmose; Mulder, Frans A A; Otzen, Daniel Erik; Arnspang, Eva C.

Published in:
Biochemistry

DOI:
10.1021/acs.biochem.3c00114

Publication date:
2023

Document version:
Accepted manuscript

Citation for pulished version (APA):
Andersen, C., Lausdahl, A. K., Nielsen, J., Clausen, M. P., Mulder, F. A. A., Otzen, D. E., & Arnspang, E. C. (2023). 4-oxo-2-nonenal-induced α-synuclein oligomers interact with membranes in the cell, leading to mitochondrial fragmentation. *Biochemistry*, *62*(16), 2417–2425. https://doi.org/10.1021/acs.biochem.3c00114

4-oxo-2-nonenal-induced α-synuclein oligomers interact with membranes in the cell, leading to mitochondrial fragmentation

Camilla B. Andersen[1,2], Astrid K. Lausdahl[2], Janni Nielsen[1], Mathias P. Clausen[2], Frans A. A. Mulder[1,3] , Daniel E. Otzen[1,4*], Eva C. Arnspang[2]*

[1] Interdisciplinary Nanoscience Center (iNANO), Gustav Wieds Vej 14, Aarhus University, 8000 Aarhus C, Denmark

[2] Department of Green Technology, SDU-Biotechnology, University of Southern Denmark, Odense, Denmark

[3] Department of Chemistry, Langelandsgade 140, Aarhus University, 8000 Aarhus C, Denmark

[4] Department of Molecular Biology and Genetics, Aarhus University, 8000 Aarhus C, Denmark

* To whom correspondence should be addressed at dao@inano.au.dk or arnspang@igt.sdu.dk

Keywords: α-synuclein; oligomers; in-cell NMR; mitochondria; lipid peroxidation products

Abbrevations: α-syn, α-synuclein; αSOs, α-syn oligomers; HNE, 4-hydroxynonenal; HSQC, Heteronuclear Single Quantum Coherence; ONE, 4-oxo-2-nonenal; PD, Parkinson's Disease; ROS, reactive oxidative species; STED, stimulated emission depletion; WB, Western blots

ABSTRACT

Oxidative stress and formation of cytotoxic oligomers by the natively unfolded protein α-synuclein (α-syn) are both connected to the development of Parkinson's Disease. This effect has been linked to lipid peroxidation and membrane disruption, but the specific mechanisms behind these phenomena remain unclear. To address this, we have prepared α-syn oligomers (αSOs) *in vitro* in the presence of the lipid peroxidation product 4-oxo-2-nonenal and investigated their interaction with live cells using in-cell NMR as well as stimulated emission depletion (STED) super-resolution and confocal microscopy. We find that the αSOs interact strongly with organellar components, leading to strong immobilization of the protein's otherwise flexible C-terminus. STED microscopy reveals that the oligomers localize to small circular structures inside the cell, while confocal microscopy shows mitochondrial fragmentation and association with both late endosome and retromer complex before the SOs interact with mitochondria. Our study provides direct evidence for close contact between cytotoxic α-syn aggregates and membraneous compartments in the cell.

INTRODUCTION

The 140-residue α-synuclein (α-syn) is the primary protein component found in amyloid deposits in the brains of patients with Parkinson's Disease (PD) and Dementia with Lewy Bodies (1). The cytotoxic species of α-syn is thought to be an α-syn oligomer (αSO) formed during α-syn self-assembly (2). Cytotoxicity has been associated with the induction of reactive oxidative species (ROS) (3) and attributed to αSO interactions with cell membranes (4-10), probably mediated by the highly structured central NAC region (residues 61-95) of the αSO (8). Membrane binding is then proposed to lead to a deregulated influx of Ca^{2+}, which together with the formation of ROS (8, 11) leads to cell death. Studies of α-syn oligomerization in live SHSY5Y cells have shown that αSOs sequester to lysosomes and that mitochondria morphology is affected (12). β-sheet-rich αSOs have also been shown to interact with mitochondria, leading to mitochondrial fragmentation and neuronal death (13). The many possible molecular mechanisms of their toxicity have been reviewed (2, 14).

Many different αSOs form *in vitro* under different conditions, though they generally share properties such as a mixture of random coil and β-sheet structure and a tendency to form a compact core with a more extended and dynamic shell (2, 15). Formation of αSO is particularly promoted by lipid peroxidation products, whose levels are elevated *in vivo* in PD (16) and therefore highly relevant to study *in vitro*. In particular the reactive aldehyde 4-oxo-2-nonenal (ONE) (17, 18) boosts α-syn oligomerization (19). The ONE-induced oligomers are rich in beta-sheet structure, and cytotoxic against *e.g.* neuroblastoma (SHSY5Y) cells (20). In a previous study the ONE-αSOs have been characterized and have showed to have similar size, morphology and toxicity as unmodified αSOs, however the ONE is able to cross link, thus making the ONE-αSOs much more stable(21). Confocal microscopy has shown that αSOs induced by another lipid peroxidation product, the aldehyde 4-hydroxynonenal (HNE) are taken up by astrocytes and oligodendrocytes and co-localize with the endo-lysosomal pathway. Strikingly, the αSOs are not degraded in the lysosomes but rather induce mitochondrial fragmentation (22). One limitation of our current insight into αSO-membrane interactions is that it is largely based on *in vitro* and model membrane studies (10). It is important to extend our observations on αSO structure, dynamics and membrane interactions to cellular conditions in order to shed further light on the mechanisms by which αSOs affect cell biology. This is the topic of the current investigation.

In-cell NMR is an emerging high-resolution technique (23) that allows us to study structural and dynamic features of proteins inside living cells. ^{15}N-isotope labeling makes it possible to study the protein inside the cell with low cellular background. Electroporation has previously been

shown to be an effective method to deliver monomeric α-syn into the cell (24), and subsequent in-cell NMR revealed that the protein thus taken up remained unstructured (24). In-cell NMR has also been used to study intracellular posttranslational modifications of α-syn such as Met oxidation (25). Yet so far, αSOs have not yet been studied with in-cell NMR. We complement this work with microscopy which in general is a highly useful methodology to study proteins *in cellula.* We use confocal laser scanning microscopy to study the distribution of αSO in side the cell and to study mitochondria in live cells. For increased image resolution, we use the super-resolution microscopy technique called stimulated emission depletion (STED), which breaks the diffraction limit (26).

Here we present the results of *in cellula* studies of ONE induced αSO using the SHSY5Y human neuroblastoma cell line. We introduce isotope-labelled αSOs into the cells by electroporation and record NMR spectra to compare their conformational properties with those of monomeric α-syn. We confirm that monomeric α-syn remains unstructured *in cellula* and largely resides in the cytosol, in dynamic interaction with cell components but with no major impact on its structure and mobility apart from small effects on the terminal regions. In contrast, the αSO interacts strongly with the cell. We elucidate cellular interactions and localization of αSOs using confocal and STED microscopy and show that the αSO interacts with different cell components and induce mitochondrial fragmentation. Thus αSOs have a central impact on cellular membranes in a biological setting.

MATERIALS AND METHODS

Details are provided in Supporting Information.

Protein preparation: Human α-syn was produced recombinantly in *E. coli*, while N-acetylated α-syn was produced by co-expression with an acetyltransferase. ^{15}N-labelled α-syn was produced by growth in minimal medium. ONE-modified αSOs were produced by co-incubation with ONE under shaking conditions followed by gel filtration.

Cell handling: SHSY5Y cells were grown in DMEM media with appropriate supplements and lysed with lysis buffer to provide cell lysates. α-syn and αSOs were electroporated into trypsinated SHSY5Y cells using a Nucleofector followed by recovery in an incubator before use for Western blotting (visualized with an anti-α-syn antibody) and microscopy. For in-cell NMR experiments, cells and growth media were supplemented with 2% melted agarose to maintain sample homogeneity.

NMR: HSQC spectra were recorded on a 950 MHz Bruker Avance spectrometer at 10^{o}C. α-syn concentration was estimated by integrating signal in the amide region for α-syn in buffer. Spectra for in-buffer and in-cell solutions were recorded under identical conditions.

Immunofluorescence microscopy: This was performed on a Zeiss LSM at 20-60x magnification with appropriate antibodies against α-syn, phalloidin and diamidino-2-phenylindole (DAPI) after fixing recovered electroporated cells with para-formaldehyde. For fragmentation analysis, mitochondria and endosomes were labelled with appropriate antibodies and samples were imaged on a Nikon A1 confocal microscope.

Live cell imaging: This was carried out on a Nikon A1 CM using mitotracker using SHSY5Y cells to which αSOs were added directly. For fragmentation analysis, mitochondria were manually classified as fragmented or tubular.

STED imaging: This was performed on an Abberior Facility Line STED microscope using cells electroporated with αSOs and subsequently fixed. For imaging we used secondary antibodies appropriate for Abberior.

RESULTS AND DISCUSSION

Monomeric α-syn remains monomeric and unstructured after transfer into SHSY5Y cells

Monomeric N-terminally acetylated ^{15}N-α-syn was delivered to SHSY5Y cells by electroporation, after which ^{15}N-edited 1D ^{1}H-NMR and ^{1}H-^{15}N-HSQC (Heteronuclear Single Quantum Coherence) spectra were recorded (Fig. S1A-C). We used N-terminally acetylated α-syn because α-syn is N-terminally acetylated in mammalian cells (24). The success of our delivery protocol and the intracellular localization of α-syn were confirmed by Western blot (WB) and immunofluorescence (Fig. S2) after the cells were trypsinized and washed to remove any extracellular α-syn. Using a dilution series, the concentration of α-syn inside the cell was estimated to 13+/-5 μM (Fig. S2A). No oligomeric form of α-syn was identified in the cell by WB (data not shown). Confocal microscopy of cells electroporated with α-syn monomer also established that the protein is found inside the electroporated cells, and that it is evenly distributed (Fig. S2B).

To confirm the concentration determination by Western blot, we used the integrated intensity of the amide region in ^{15}N-edited 1D ^{1}H-NMR spectral. Based on the integration of a spectrum of α-syn of known concentration in buffer, the cellular concentration was estimated to be 13 μM (Fig. S3A-B), in excellent agreement with the Western blot-based concentration estimate. This value corresponds well with the physiological concentration in the synapse, which is ~20 μM (27). The close correspondence of the estimates from Western blotting and NMR demonstrates that the major part of the protein is present in the cytosol.

Next, we analyzed the conformational properties of monomeric *in-cell* α-syn. The peaks of HSQC spectra of α-syn in cell show a decrease in intensity compared to buffer due to line broadening (Fig. S3C). Line broadening is common in in-cell NMR (28) and arises from non-specific interactions with cytosolic components and molecular crowding (29, 30). We also see a small offset of the chemical shift throughout the sequence and a large perturbation around His50 (Fig. S3D), but overall the changes are minimal and indicate that α-syn is just as unfolded inside the cell as *in vitro*, in good agreement with previous observations (24). We ascribe the shift of His50 to a change in the side-chain protonation state of His50 in the cytosol compared to buffer. His50 is known to increase its pK_a value when α-syn is bound to the negatively charged SDS-micelles, similar effect may be present when interacting with lipid cell membranes (31). H50Q mutations have been described in familial cases of PD promoting α-Syn aggregation and therefore His50 interaction with the membrane is of great interest. The interaction of the disease variant H50Q has not shown to change the interaction of α-syn with membranes when using SUV as model (32), however the effect could be interesting to study with in-cell NMR. In spite of the random coil characteristics of monomeric α-syn, as well as the lack of alternative states such as αSOs according to WB, there is a decrease in in-cell intensity due to line broadening. This probably reflects the crowded environment in the cell, which reduces α-syn mobility. The reduction in intensity is largest for the termini. Our data confirm the observations by Theillet et al (24) who attributed these to weak hydrophobic interactions between the N-terminus and the membrane, while the reduction in the C-terminal intensity was ascribed to weak electrostatic interactions (24).

NMR spectra of in-cell αSOs show significant changes compared to buffer

We then turned to ^{15}N-labelled αSOs, which had been prepared in the presence of ONE to increase their stability and reduce dissociation into monomers (21). The αSOs were prepared by incubation of 200 μM α-syn in PBS solution in the presence of 0.8 mM ONE for 24h, followed be removal of residual monomer and unreacted ONE by size exclusion chromatography (SEC) purification, the kinetics of this process has been analyzed previously and the above incubation time and concentration has been found to be optimal (21). The oligomeric sample was electroporated into SHSY5Y cells, and ^{1}H-^{15}N-HSQC spectra were recorded of the cell suspension after a recovery time of 5 hours (Fig. S4B). It was not possible to estimate the αSO concentration in the cell by NMR, due to the low signal from αSOs in the cell. However, Western blotting gave an estimated concentration of 9+/-5 μM in monomer equivalents (Fig. 1A), which is very similar to that of monomeric α-syn. Fluorescence

microscopy confirmed the presence of the αSO inside the cells (Fig. 1B). Nevertheless, confocal fluorescence images of the cells after electroporation highlight a different distribution pattern for oligomers versus monomers. Whereas monomeric α-syn is distributed evenly throughout the cell, including the nucleus, the αSO is mainly in the cytoplasm and close to the cell membrane. Furthermore, αSOs form more punctate-like aggregates than monomers (Fig. 2).

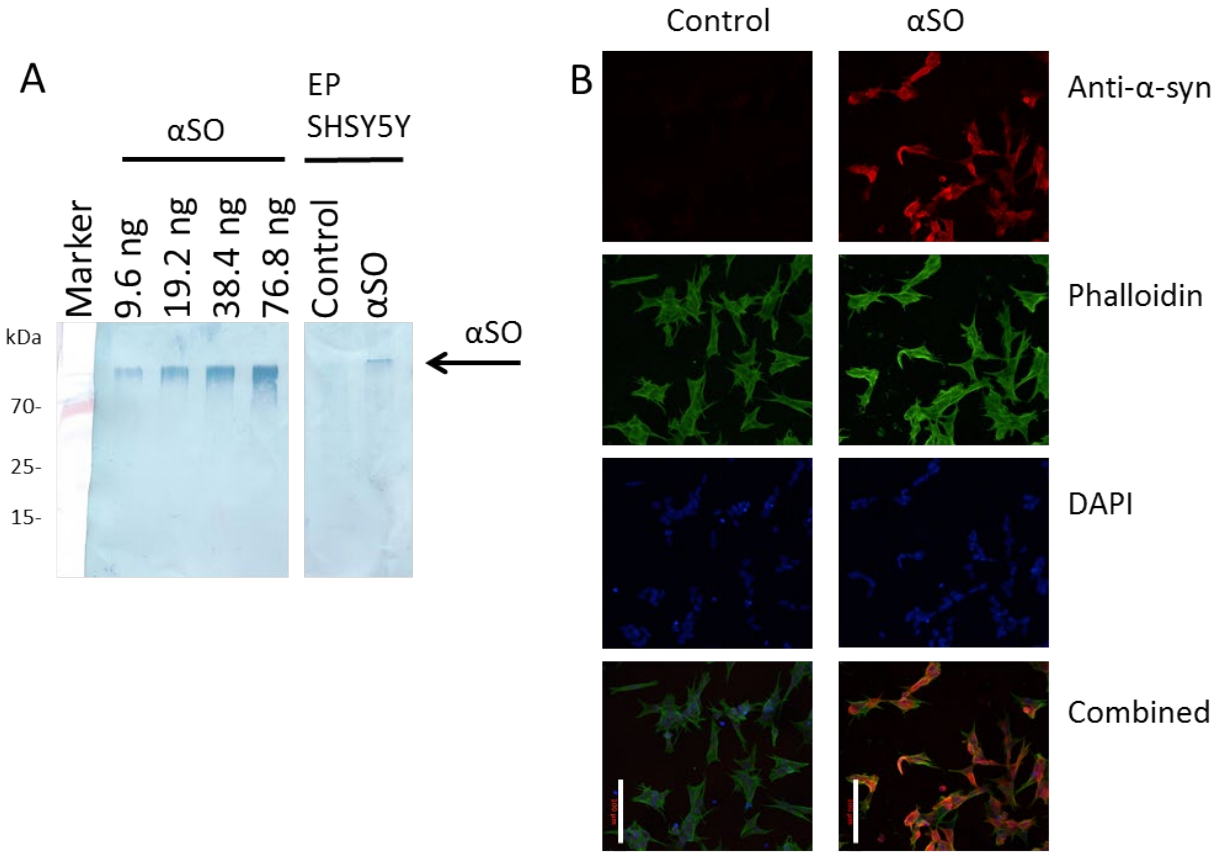

Figure 1: **Fluorescence microscopy and WB of SHSY5Y cells electroporated with αSO.** A: Western blot of electroporated (EP) cells and dilution series of αSO in buffer. B: Fluorescence microscopy of SHSY5Y cells electroporated with αSO or (buffer) control. Red: α-syn (anti-α-syn), green: actin (Phalloidin), blue: nuclei (DAPI). Length of scale bar is 100 µm.

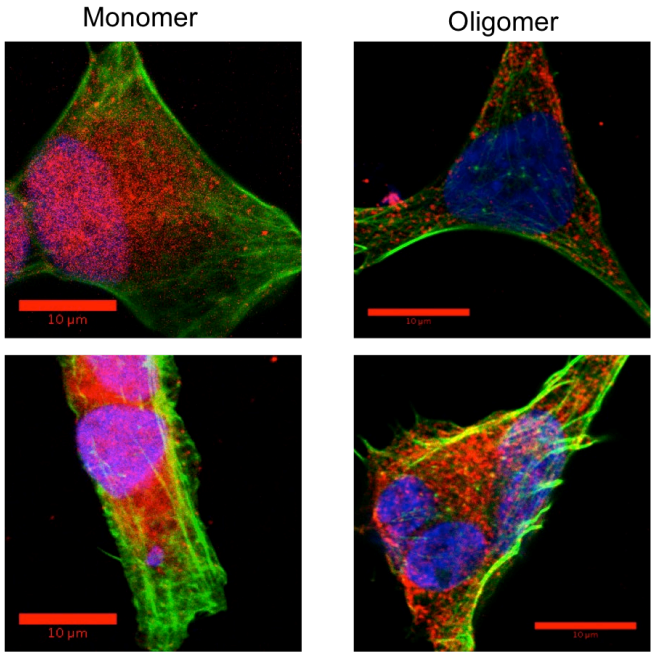

Figure 2: Comparison of confocal microscopy of cells with monomer and oligomer. SHSY5Y cells electroporated with monomer (left) and αSO (right). Red: α-syn (anti-α-syn), green: actin (Phalloidin), blue: nuclei (DAPI). Scalebar 10 µm.

Unlike the case for monomeric α-syn, there is hardly any NMR signal from the αSO inside cells (Fig. 3A-B, Fig. S4A-B). Although the entire C-terminal tail of αSO (residues 60-100) is flexible and visible by NMR in buffer (Fig. S4), as reported previously (33), the in-cell spectrum of the αSO only reveals four peaks (in addition to a few cellular metabolite peaks). Furthermore, these peaks do not superimpose with αSO peaks in buffer. In spite of the peak displacement, it is to be expected that the observed peaks are from the C-terminal residues and the strong signal in the bottom right is therefore most likely due to Ala140, the C-terminal residue of α-syn. The remaining 3 peaks are assigned based on the assumption that peak intensity will decline monotonically as we move away from the C-terminus, just as is seen for the αSO in buffer (33). It also appears self-evident that all highly mobile residues should be connected in sequence in this region of the protein. In this way, we assign the peaks in rank of declining intensity to E139, E137 and Y136 (P138 is not visible in ^{15}N-^{1}H-HSQC spectra as it lacks an amide hydrogen). In turn, the significant chemical shift perturbation (CSP) of A140 suggests that sequentially linked residues should also undergo significant CSP. Indeed, the CSP of the 3 remaining peaks is also significant (Fig. 3C), indicating a change in the chemical environment of these residues compared to *in vitro* conditions. Possible degradation of αSO

should also be taken into account when interpreting the NMR results. NMR of α-syn in SHSY5Y cells has shown proteolytic C-terminal truncation leading to new NMR signals after prolonged recovery times (12 hrs) . The new peak observed here coming from A140, could resemble the peak which appears after such degradation. However, in the present study cells were only subjected to 5 hrs recovery after electroporation, and the rest of the peaks are not similar to those found due to proteolysis. Nevertheless, more studies of intracellular oligomer should be done to be able to rule out proteolysis (34).

The decrease in intensity and disappearance of peaks suggest that α-syn's otherwise highly dynamic C-terminus is largely immobilized. The N-terminal region is known to be very important for interactions with membranes for both monomeric α-syn and αSOs (5, 8). By solid state NMR it has been shown that toxic αSOs insert into membranes via the NAC-region, mediated by interaction with the N-terminal to the surface of the membrane (8). Our data indicate that the C-terminus is also affected by this interaction, possibly because the core of the αSO interacts closely with the hydrophobic part of the membrane, forging interactions of the C-terminus with the membrane surface.

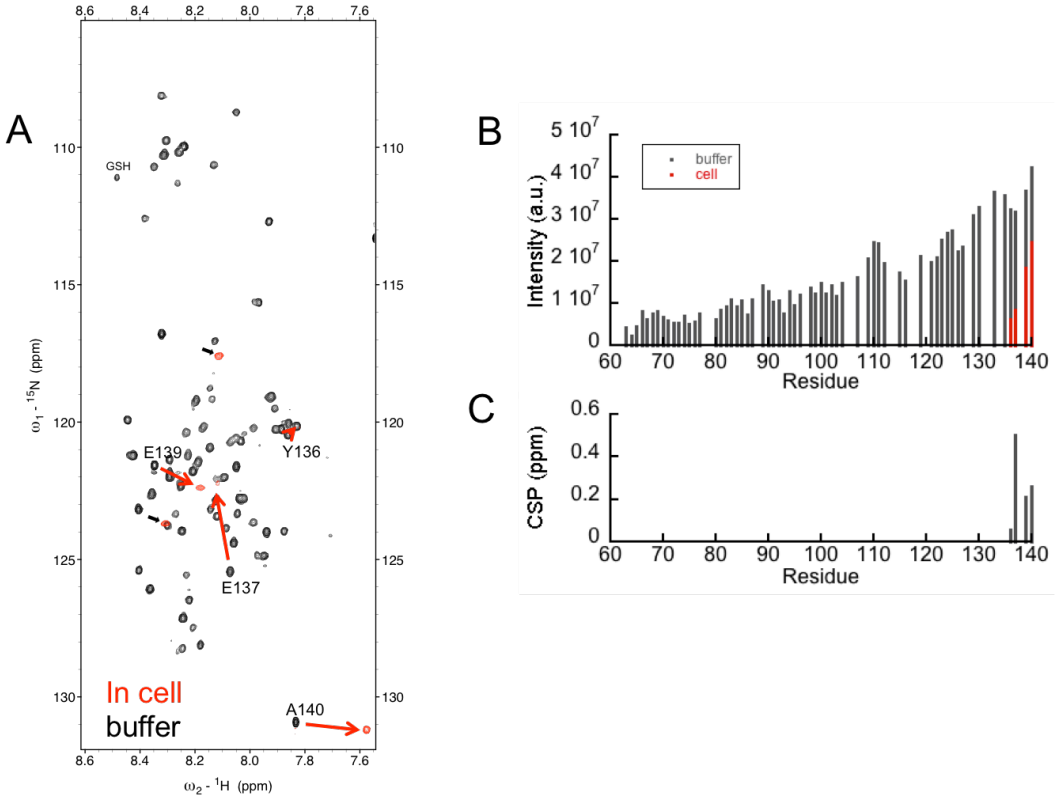

Figure 3: in-cell NMR of SHSY5Y cells electroporated with αSO. A: ^{1}H-^{15}N-HSQC of αSO in cell (red) and αSO in buffer (black). Small black arrows denote growth medium-specific metabolite signals (background). Big red arrows indicate proposed chemical shift changes for peaks in the in-cell sample. B: Intensity of peaks in ^{1}H-^{15}N-HSQC spectra (in A) of αSO in buffer (black) and in cell (red). The intensity is weighted with the concentration of the αSO (by WB quantification). C: chemical shift perturbation (CSP).

αSOs interact differently with whole cells and cell lysate

To elucidate the basis for the reduction in NMR signal intensity from αSO, we also recorded spectra of αSOs in the presence of whole live cells (without electroporation, *i.e.* only cellular contact via the membrane and through spontaneous translocation, as previously reported (20)), cell lysate (*i.e.* a diluted cellular environment with increased access to the different compartments and membranes) and cell media. The signals of the non-electroporated samples are overall significantly greater than those of the in-cell αSO in the ranking order media > cell lysate > whole cells. Remarkably, if the cell lysate is centrifuged to remove the nuclei, mitochondria and cellular debris, the signal is restored to 100% of the intensity in media (Fig. 4), indicating that binding to these cellular elements accounts for almost all the decrease in signal. For monomeric α-syn, a similar pattern in signal can be recognized when binding to lipids. There, an increasing amount of anionic lipid initially decreases the signal from N-terminus followed by the NAC region up to around residue 97 (35, 36), while the C-terminal region remains visible throughout.

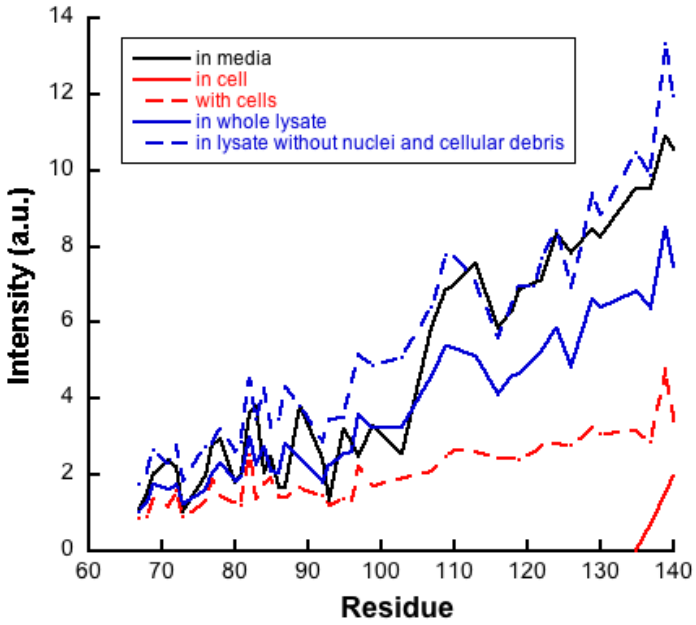

Figure 4: NMR of 15N-αSOs in different environment. ^{1}H-^{15}N-HSQC of the αSOs in media (black), in SHSY5Y cells (in-cell NMR sample from figure 3) (red), with SHSY5Y cells (whole live cells in media, no electroporation) (dotted red), cell lysate (blue) and in lysate centrifuged to remove cell debris, mitochondria and nucleus (dotted blue).

αSOs increase mitochondrial fragmentation

Our in-cell NMR data were consistent with interactions between αSOs and mitochondria. It has been reported in several *in vitro* and *in vivo* studies that αSOs interact with membranes (4-9), and mitochondrial fragmentation by αSO has been reported indicating a role for αSO in mitochondrial dysfunction in PD (12, 22). To extend our NMR data, we therefore turned to confocal microscopy of SHSY5Y electroporated with αSO (Fig. 5A). Since electroporation is known to damage the mitochondrial membrane (37), a mock experiment with buffer alone was also included. The images revealed that mitochondria of electroporated cells formed a range of morphologies, spanning from short fragments to tubular network as in healthy cells (38). Comparing the images from the cells treated with αSO versus buffer revealed a significant increase in fragmentation of their mitochondria (Fig. 5B). The confocal images furthermore revealed that the amount of αSO varied greatly among cells in the same sample (and same image) (Fig. S5).

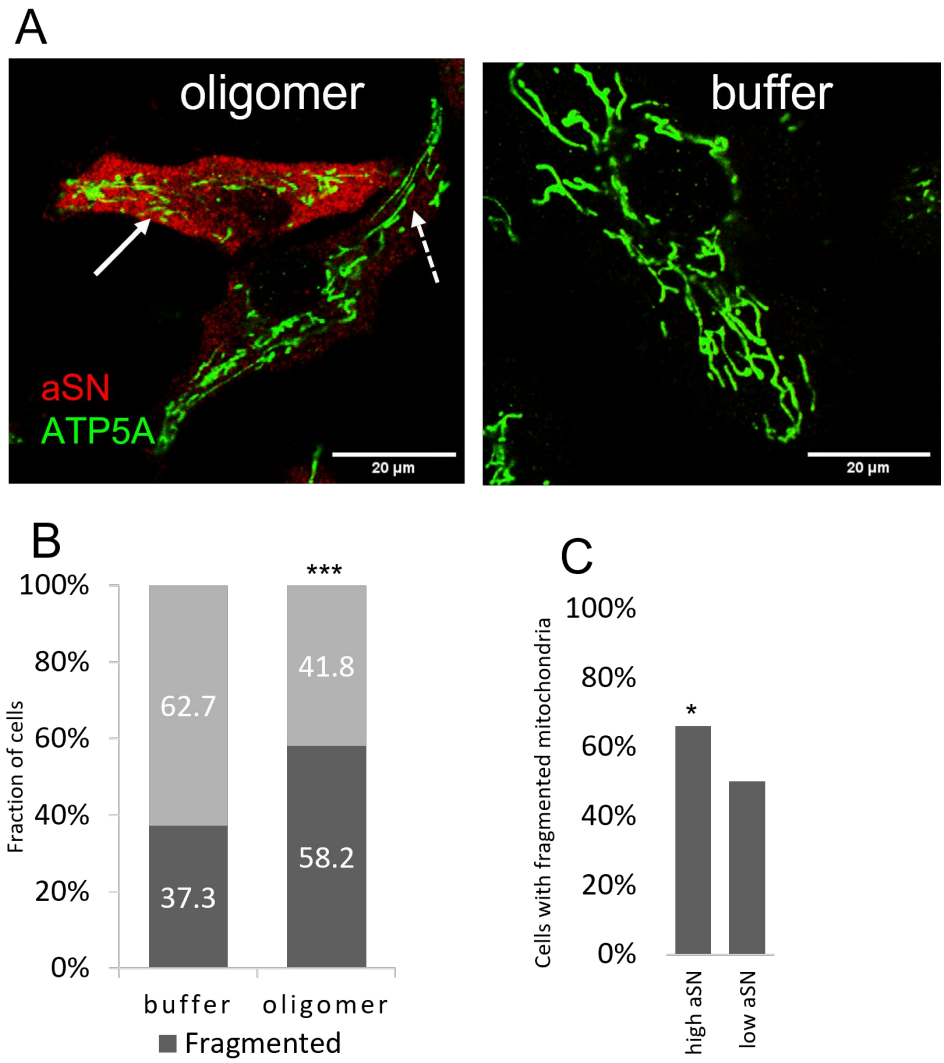

Figure 5: Mitochondrial fragmentation analysis. A: Confocal image of SHSY5Y cells electroporated with αSO (left) or buffer (right) and stained with anti-α-syn (red) and anti-ATP5A (green, mitochondria membrane). Solid arrow points to fragmented mitochondria and dashed arrow to tubular mitochondria. B: Number of cells with fragmented mitochondria versus tubular mitochondria. Statistical test: z-test, difference between number of fragmented mitochondria in samples with treated cells (n=169) vs mock (n=165). Two tailed, ***: $p \leq 0.0001$. C: The fragmentation fraction in cells with high and low amount of α-syn (specified with an intensity threshold) for sample electroporated with oligomer. Statistical test: z-test, difference between number of fragmented mitochondria in high vs low α-syn cells. Two tailed, *: $p \leq 0.05$ (n=152).

To take these variations in the samples into account and correlate the fragmentation of mitochondria with the amount of αSO inside the cell, the cells were binned to either "high α-syn" or "low α-syn" based on mean intensity of signal from αSO in the cytoplasm and a defined threshold.

This showed a significantly higher number of cells with fragmented mitochondria among the cells with high amounts of α-syn (Fig. 5C). Therefore, we conclude that the fragmentation of mitochondria is due to the presence of αSOs. This is consistent with studies reporting fragmentation of mitochondria by different types of αSOs induced by dopamine, overexpression of α-syn (wt and mutants) and fibril seeds, respectively (12, 39, 40).

We further investigated the fragmentation of mitochondria by studying the fragmentation of mitochondria in live cells without electroporation. Here αSO was added to the media surrounding the cells, and the fragmentation of mitochondria was followed under the microscope using MitoTracker (Fig. S6). The lengths of the mitochondria were then quantified after incubation with αSO for 1h and again an hour later (Fig. 6 A-B). To take laser toxicity into account, control cells without αSO were also quantified. We did not see any significant mitochondrial fragmentation in control cells. However, we did see a dose-dependent decrease in mitochondria length with αSO concentration (Fig. 6C). This shows that αSO uptake from media can induce the fragmentation similar to what was observed after electroporation of αSO into the cell.

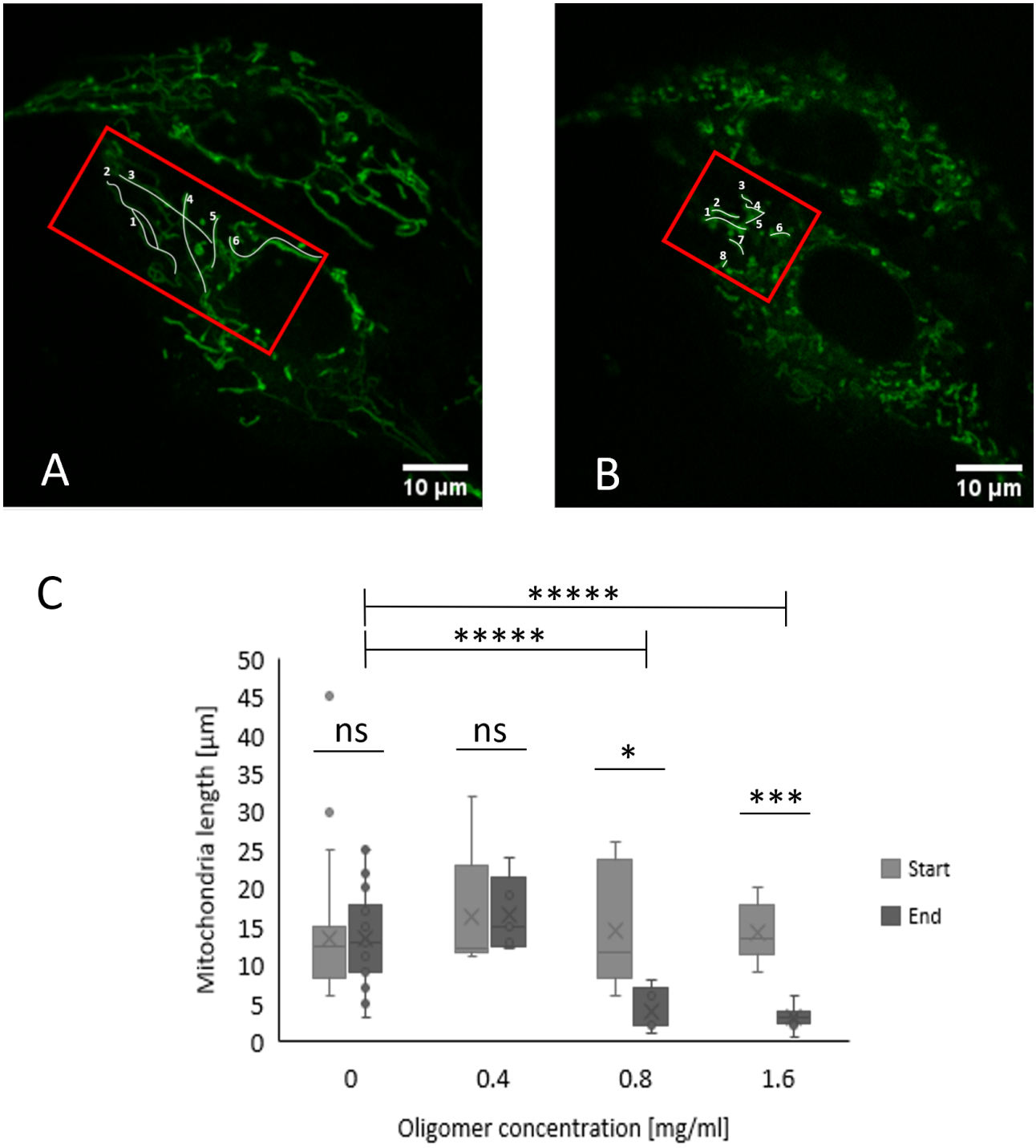

Figure 6: Quantification of mitochondria lengths in live cell imaging. A-B: Example of mitochondria measurements. A: image of cells 1 h after addition of 1.6 mg/ml αSO, B: image of cell 2 h after addition of 1.6mg/ml. The red box shows ROI and white lines shows measurements. C: Boxplot of mitochondria lengths in cells treated with 0, 0.4, 0.8 and 1.6 mg/ml oligomer. Statistical test: students t-test, Two tailed, *:p≤0.05,

***: p≤0.001, *****: p≤0.00001. The two top bars compare the end-value at 0 mg/ml αSO with end-values at 0.8 and 1.6 mg/ml, respectively.

αSOs show promiscuous binding

In order to investigate the αSO localization in the cell in greater detail, we turned to super-resolution microscopy using STED. Cells were fixed after 5 hrs to image the cells at the same time scale as cells studied with NMR. The cells were stained with anti-ATP5A to image mitochondria and anti-α-syn to stain oligomer. STED imaging showed that αSOs form remarkably regular circular structures which did not co-localize with mitochondria (Fig. 7). This correlates well with dSTORM imaging by Aartsma and coworkers which showed that α-syn amyloid aggregates localize with endocytotic vesicles (41). It has also been shown that α-syn monomers colocalize with markers for late endosome/lysozyme Rab7 and the retromer protein VPS35 in brain endothelial cells after uptake from media (42). Furthermore, mitochondrial fragmentation has been observed in a PD disease mouse model with a heterozygous (D620N) mutation of Vacuolar Protein Sorting 35 (VPS35) (43). PD with disease mutation D620N VPS35 resembles sporadic PD, indicating that common mechanisms may underlie both familial and sporadic PD (44). Therefore, we tested the co-localization of the αSO with these markers after uptake of αSO from the media without electroporation.

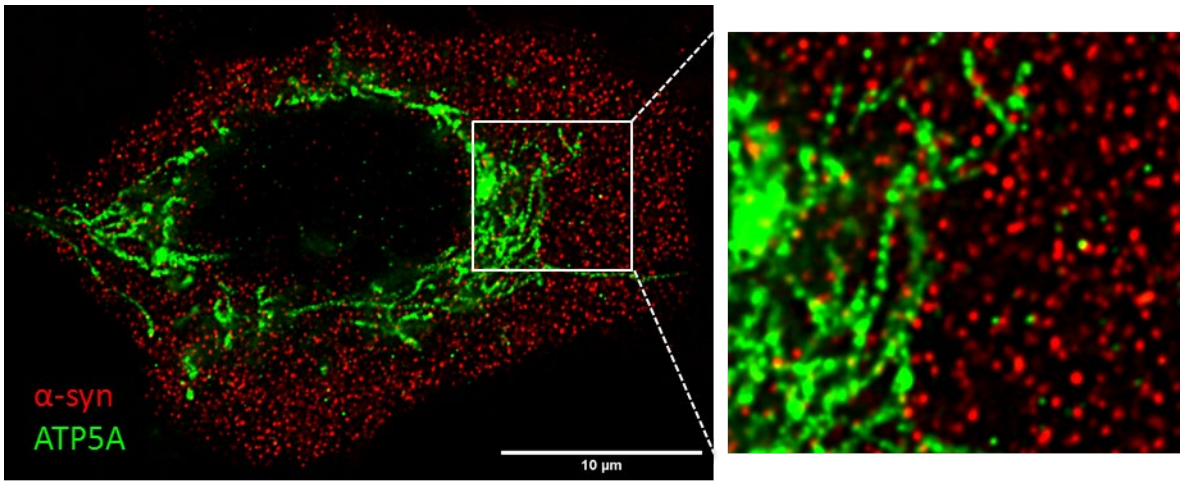

Figure 7: STED imaging of SHSY5Y cells with αSO. The sample is stained to visualize α-syn (red) and ATP5A (green, mitochondria). Inset to the left is a zoom of the highlighted area.

Co-localization was investigated after 10 min and 5 h after addition to the media. The colocalization with ATP5A (mitochondria), Rab7 (late endosome) and VPS35 (retromer) was

quantified using Pearson's correlations coefficient (Fig. 8). The correlation coefficient is very low for all three. This could be due to the fact that the αSOs do not co-localize to only one cellular membrane/protein but will have multiple binding partners in the cell and therefore not have strong correlation to only one. Other potential targets for αSO include chaperones and the proteasome (45, 46). However, we observe a significant change in Pearson's correlation coefficient over time. For Rab7 and VPS35, the highest correlation is in the first time point (10 min) whereas the ATP5A has the highest correlation at the later time point (5h) indicating that the αSO uptake is through the endo-lysosomal pathway and some of the αSO is then ending up at the mitochondrial membrane. This agrees well with the Erlandsson group's work with HNE-induced αSOs (22). To further increase the resolution of the co-localization study STED could be used for future studies and followed at several time points.

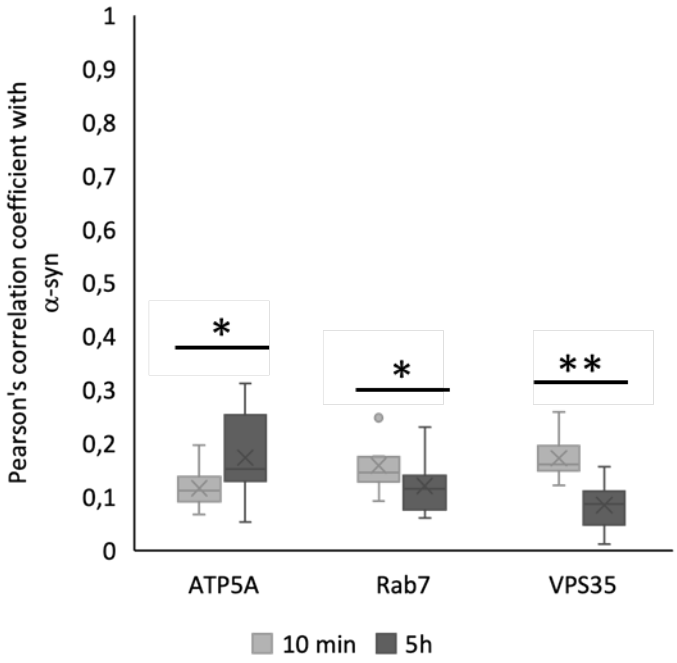

Figure 8: co-localization analysis of αSO with ATP5A, Rab7 and VPS35: Boxplot of Pearson's correlation coefficient. The statistical test used was a two-sided, unpaired Mann-Whitney test (*$p < 0.05$ and ** $p< 0.01$).

The toxicity of the αSOs is thought to be due to disruption of the integrity of the cellular membrane and an increase in the production of ROS and lipid peroxidation products. This leads to a decrease in cell viability, but also the possibility of further increase in formation of toxic αSOs (47). The αSOs studied in this paper are formed and stabilized due to the interaction with ONE, a lipid peroxidation product. Not only is the αSO formation based on interaction with lipid peroxidation product but the

subsequent toxicity of the αSO is due to interaction with lipid membranes (48). The increased oxidative stress observed in PD can lead to ROS formation which in turn can initiate lipid peroxidation and formation of ONE, promoting increased αSO formation. Simultaneously αSOs has shown to increase ROS levels (47) as a positive feedback loop. However, PD is a complex disease where aggregation of α-syn is influenced by multiple factors of which ROS only form one part. To increase the understanding of ONE- αSOs effect studied in this paper additional assay such as Ca^{2+} and ROS assays as used by Fani et al . 2022 could be employed, They found that Aβ-oligomer led to increase in Ca2+ which caused the increase in ROS (49). Furthermore, the effect of ONE-αSOs compared to protofibrils could be interesting to study as they are expected to have different effects in the propagation of PD (2).

In-cell NMR combined with microscopy as used in this study has the potential to increase our understanding of the neuroprotective role of molecules potentially inhibiting the cytotoxic properties of the oligomeric species within our growing collection of antibodies, peptides and small molecules binding to the α-syn oligomer.

In summary, the assembly of α-syn into αSOs increases the interaction between different cellular membranes and α-syn and this also affects the C-terminus of α-syn. In this study we investigated the interaction of αSOs with the membrane at atomic resolution in live cells. We show that ONE-induced αSO interactions with the cell lead to mitochondrial fragmentation, which could be due to direct interaction with the mitochondria as ONE-induced oligomers are able to permabilize membranes *in vitro* (21). αSO induced by overexpression has also been shown to interact directly with mitochondrial membranes (50, 51). The fragmentation could also be due to interactions between αSO and the endo-lysosomal system, leading to perturbation of cellular homeostasis. Specifically deficiency in the retromer protein VPS35 can lead to the mitochondrial fragmentation observed (52). These oberservations opens for further study of αSO interaction with the endo-lysosomal system in cell to find strategies to ultimately treat PD. The mechanism of αSOs interaction with the cell and how the toxicity is induced by αSOs, is important to understand in relation to finding therapeutics towards PD.

SUPPORTING INFORMATION

Detailed description of preparation of recombinant α-syn and ONE-modified αSOs, cell line growth, cell lysate preparation, electroporation of recombinant α-syn into mammalian cells, Western blots, immunofluorescence microscopy, in-cell NMR, Live cell imaging with Mitotracker, image analysis and STED analysis. Figures showing in-cell NMR and microscopy data for monomer α-syn and individual ^{15}N-^{1}H HSQC spectra of α-syn monomer and αSO in cell and in buffer and of SHSY5Y cells. Example of confocal images used in fragmentation quantification (PDF). Video of cell with Mitotracker after αSO addition (.avi file).

ACKNOWLEDGEMENTS

This work was performed using the NMR spectrometers at the Danish Center for Ultra-High Field NMR Spectroscopy (Ministry of Higher Education and Science grant AU-2010-612-181). Image acquisitions were performed at the Danish Molecular Biomedical Imaging Center (DaMBIC, University of Southern Denmark). We thank Phillip Selenko and his lab for generous help and advice on in-cell NMR and electroporation and Poul Henning Jensen for kindly providing SHSY5Y cells.

FUNDING SOURCES

This work is generously supported by The Independent Research Fund Denmark | Medical Sciences (grant number 4183-00225), Grosserer L.F. Foghts Fond (grant 21.178 to acquire a Nucleofector) and the Lundbeck Foundation (grant number R276-2018-671) to D.E.O. and a Villum Young Investigator grant (grant number 19105) to E.A.C.

REFERENCES

1. Spillantini, M. G., Crowther, R. A., Jakes, R., Hasegawa, M., andGoedert, M. (1998) alpha-synuclein in filamentous inclusions of Lewy bodies from Parkinson's disease and dementia with Lewy bodies P Natl Acad Sci USA **95**, 6469-6473 DOI 10.1073/pnas.95.11.6469
2. Alam, P., Bousset, L., Melki, R., andOtzen, D. E. (2019) alpha-synuclein oligomers and fibrils: a spectrum of species, a spectrum of toxicities J Neurochem **150**, 522-534 10.1111/jnc.14808
3. Cremades, N., Cohen, S. I., Deas, E., Abramov, A. Y., Chen, A. Y., Orte, A. *et al.* (2012) Direct observation of the interconversion of normal and toxic forms of alpha-synuclein Cell **149**, 1048-1059 10.1016/j.cell.2012.03.037
4. Winner, B., Jappelli, R., Maji, S. K., Desplats, P. A., Boyer, L., Aigner, S. *et al.* (2011) In vivo demonstration that alpha-synuclein oligomers are toxic Proc Natl Acad Sci U S A **108**, 4194-4199 10.1073/pnas.1100976108
5. Lorenzen, N., Lemminger, L., Pedersen, J. N., Nielsen, S. B., andOtzen, D. E. (2014) The N-terminus of alpha-synuclein is essential for both monomeric and oligomeric interactions with membranes Febs Lett **588**, 497-502 10.1016/j.febslet.2013.12.015
6. Danzer, K. M., Haasen, D., Karow, A. R., Moussaud, S., Habeck, M., Giese, A. *et al.* (2007) Different species of alpha-synuclein oligomers induce calcium influx and seeding J Neurosci **27**, 9220-9232 10.1523/Jneurosci.2617-07.2007
7. Lashuel, H. A., Hartley, D., Petre, B. M., Walz, T., andLansbury, P. T. (2002) Neurodegenerative disease - Amyloid pores from pathogenic mutations Nature **418**, 291-291 DOI 10.1038/418291a
8. Fusco, G., Chen, S. W., Williamson, P. T. F., Cascella, R., Perni, M., Jarvis, J. A. *et al.* (2017) Structural basis of membrane disruption and cellular toxicity by alpha-synuclein oligomers Science **358**, 1440-1443 10.1126/science.aan6160
9. Volles, M. J., Lee, S. J., Rochet, J. C., Shtilerman, M. D., Ding, T. T., Kessler, J. C. *et al.* (2001) Vesicle permeabilization by protofibrillar α-synuclein: implications for the pathogenesis and treatment of Parkinson's disease Biochemistry **40**, 7812-7819,
10. Musteikyte, G., Jayaram, A. K., Xu, C. K., Vendruscolo, M., Krainer, G., andKnowles, T. P. J. (2021) Interactions of alpha-synuclein oligomers with lipid membranes Biochim Biophys Acta Biomembr **1863**, 183536 10.1016/j.bbamem.2020.183536
11. Angelova, P. R., Ludtmann, M. H., Horrocks, M. H., Negoda, A., Cremades, N., Klenerman, D. *et al.* (2016) Ca2+ is a key factor in alpha-synuclein-induced neurotoxicity Journal of cell science **129**, 1792-1801 10.1242/jcs.180737
12. Plotegher, N., Gratton, E., andBubacco, L. (2014) Number and Brightness analysis of alpha-synuclein oligomerization and the associated mitochondrial morphology alterations in live cells Biochim Biophys Acta **1840**, 2014-2024 10.1016/j.bbagen.2014.02.013
13. Ludtmann, M. H. R., Angelova, P. R., Horrocks, M. H., Choi, M. L., Rodrigues, M., Baev, A. Y. *et al.* (2018) α-synuclein oligomers interact with ATP synthase and open the permeability transition pore in Parkinson's disease Nature Communications **9**, 2293 10.1038/s41467-018-04422-2
14. Roberts, H. L., andBrown, D. R. (2015) Seeking a mechanism for the toxicity of oligomeric alpha-synuclein Biomolecules **5**, 282-305 10.3390/biom5020282

15. van Diggelen, F., Tepper, A. W. J. W., Apetri, M. M., andOtzen, D. E. (2017) α-Synuclein Oligomers: A Study in Diversity Israel Journal of Chemistry **57**, 699-723 doi:10.1002/ijch.201600116
16. Dexter, D. T., Carter, C. J., Wells, F. R., Javoy-Agid, F., Agid, Y., Lees, A. *et al.* (1989) Basal Lipid Peroxidation in Substantia Nigra Is Increased in Parkinson's Disease Journal of Neurochemistry **52**, 381-389 doi:10.1111/j.1471-4159.1989.tb09133.x
17. Rindgen, D., Nakajima, M., Wehrli, S., Xu, K., andBlair, I. A. (1999) Covalent modifications to 2'-deoxyguanosine by 4-oxo-2-nonenal, a novel product of lipid peroxidation Chem Res Toxicol **12**, 1195-1204, https://www.ncbi.nlm.nih.gov/pubmed/10604869
18. Lee, S. H. (2000) Characterization of 4-Oxo-2-nonenal as a Novel Product of Lipid Peroxidation Chemical research in toxicology **13**, 698-702 10.1021/tx000101a
19. Nasstrom, T., Wahlberg, T., Karlsson, M., Nikolajeff, F., Lannfelt, L., Ingelsson, M. *et al.* (2009) The lipid peroxidation metabolite 4-oxo-2-nonenal cross-links alpha-synuclein causing rapid formation of stable oligomers Biochem Biophys Res Commun **378**, 872-876 10.1016/j.bbrc.2008.12.005
20. Nasstrom, T., Fagerqvist, T., Barbu, M., Karlsson, M., Nikolajeff, F., Kasrayan, A. *et al.* (2011) The lipid peroxidation products 4-oxo-2-nonenal and 4-hydroxy-2-nonenal promote the formation of alpha-synuclein oligomers with distinct biochemical, morphological, and functional properties Free Radic Biol Med **50**, 428-437 10.1016/j.freeradbiomed.2010.11.027
21. Andersen, C., Gronnemose, A. L., Pedersen, J. N., Nowak, J. S., Christiansen, G., Nielsen, J. *et al.* (2021) Lipid Peroxidation Products HNE and ONE Promote and Stabilize Alpha-Synuclein Oligomers by Chemical Modifications Biochemistry **60**, 3644-3658 10.1021/acs.biochem.1c00478
22. Lindström, V., Gustafsson, G., Sanders, L. H., Howlett, E. H., Sigvardson, J., Kasrayan, A. *et al.* (2017) Extensive uptake of α-synuclein oligomers in astrocytes results in sustained intracellular deposits and mitochondrial damage Molecular and Cellular Neuroscience **82**, 143-156 https://doi.org/10.1016/j.mcn.2017.04.009
23. Luchinat, E., andBanci, L. (2017) In-cell NMR: a topical review IUCrJ **4**, 108-118 10.1107/S2052252516020625
24. Theillet, F. X., Binolfi, A., Bekei, B., Martorana, A., Rose, H. M., Stuiver, M. *et al.* (2016) Structural disorder of monomeric alpha-synuclein persists in mammalian cells Nature **530**, 45-50 10.1038/nature16531
25. Binolfi, A., Limatola, A., Verzini, S., Kosten, J., Theillet, F. X., Rose, H. M. *et al.* (2016) Intracellular repair of oxidation-damaged alpha-synuclein fails to target C-terminal modification sites Nat Commun **7**, 10251 10.1038/ncomms10251
26. Klar, T. A., Jakobs, S., Dyba, M., Egner, A., andHell, S. W. (2000) Fluorescence microscopy with diffraction resolution barrier broken by stimulated emission Proc Natl Acad Sci U S A **97**, 8206-8210 10.1073/pnas.97.15.8206
27. Wilhelm, B. G., Mandad, S., Truckenbrodt, S., Kroehnert, K., andSchaefer, C. (2014) Composition of isolated synaptic boutons reveals the amounts of vesicle trafficking proteins Science (New York, NY) **344**, 1023-1028 10.1126/science.1252884
28. Lippens, G., Cahoreau, E., Millard, P., Charlier, C., Lopez, J., Hanoulle, X. *et al.* (2018) In-cell NMR: from metabolites to macromolecules Analyst **143**, 620-629 10.1039/C7AN01635B

29. Crowley, P. B., Chow, E., andPapkovskaia, T. (2011) Protein interactions in the Escherichia coli cytosol: an impediment to in-cell NMR spectroscopy Chembiochem **12**, 1043-1048 10.1002/cbic.201100063
30. Pastore, A., andTemussi, P. A. (2017) The Emperor's new clothes: Myths and truths of in-cell NMR Archives of Biochemistry and Biophysics **628**, 114-122 https://doi.org/10.1016/j.abb.2017.02.008
31. Croke, R. L., Patil, S. M., Quevreaux, J., Kendall, D. A., andAlexandrescu, A. T. (2011) NMR determination of pKa values in alpha-synuclein Protein Sci **20**, 256-269 10.1002/pro.556
32. Khalaf, O., Fauvet, B., Oueslati, A., Dikiy, I., Mahul-Mellier, A. L., Ruggeri, F. S. *et al.* (2014) The H50Q mutation enhances alpha-synuclein aggregation, secretion, and toxicity J Biol Chem **289**, 21856-21876 10.1074/jbc.M114.553297
33. Lorenzen, N., Nielsen, S. B., Yoshimura, Y., Vad, B. S., Andersen, C. B., Betzer, C. *et al.* (2014) How Epigallocatechin Gallate Can Inhibit alpha-Synuclein Oligomer Toxicity in Vitro Journal of Biological Chemistry **289**, 21299-21310 10.1074/jbc.M114.554667
34. Limatola, A., Eichmann, C., Jacob, R. S., Ben-Nissan, G., Sharon, M., Binolfi, A. *et al.* (2018) Time-Resolved NMR Analysis of Proteolytic alpha-Synuclein Processing in vitro and in cellulo Proteomics **18**, e1800056 10.1002/pmic.201800056
35. Viennet, T., Wordehoff, M. M., Uluca, B., Poojari, C., Shaykhalishahi, H., Willbold, D. *et al.* (2018) Structural insights from lipid-bilayer nanodiscs link alpha-Synuclein membrane-binding modes to amyloid fibril formation Commun Biol **1**, 44 10.1038/s42003-018-0049-z
36. Das, T., Acosta, D., andEliezer, D. (2020) Interactions of IDPs with Membranes Using Dark-State Exchange NMR Spectroscopy Methods Mol Biol **2141**, 585-608 10.1007/978-1-0716-0524-0_30
37. Batista Napotnik, T., Polajžer, T., andMiklavčič, D. (2021) Cell death due to electroporation – A review Bioelectrochemistry **141**, 107871 https://doi.org/10.1016/j.bioelechem.2021.107871
38. Frazier, A. E., Kiu, C., Stojanovski, D., Hoogenraad, N. J., andRyan, M. T. (2006) Mitochondrial morphology and distribution in mammalian cells **387**, 1551-1558 doi:10.1515/BC.2006.193
39. Prots, I., Grosch, J., Brazdis, R.-M., Simmnacher, K., Veber, V., Havlicek, S. *et al.* (2018) alpha-Synuclein oligomers induce early axonal dysfunction in human iPSC-based models of synucleinopathies Proceedings of the National Academy of Sciences **115**, 7813-7818 doi:10.1073/pnas.1713129115
40. Grassi, D., Howard, S., Zhou, M., Diaz-Perez, N., Urban, N. T., Guerrero-Given, D. *et al.* (2018) Identification of a highly neurotoxic α-synuclein species inducing mitochondrial damage and mitophagy in Parkinson's disease Proc Natl Acad Sci U S A **115**, E2634-e2643 10.1073/pnas.1713849115
41. Apetri, M. M., Harkes, R., Subramaniam, V., Canters, G. W., Schmidt, T., andAartsma, T. J. (2016) Direct Observation of α-Synuclein Amyloid Aggregates in Endocytic Vesicles of Neuroblastoma Cells PLOS ONE **11**, e0153020 10.1371/journal.pone.0153020
42. Alam, P., Holst, M. R., Lauritsen, L., Nielsen, J., Nielsen, S. S. E., Jensen, P. H. *et al.* (2022) Polarized alpha-synuclein trafficking and transcytosis across brain endothelial cells via Rab7-decorated carriers Fluids Barriers CNS **19**, 37 10.1186/s12987-022-00334-y
43. Chiu, C. C., Weng, Y. H., Huang, Y. Z., Chen, R. S., Liu, Y. C., Yeh, T. H. *et al.* (2020) (D620N) VPS35 causes the impairment of Wnt/beta-catenin signaling cascade and

mitochondrial dysfunction in a PARK17 knockin mouse model Cell Death Dis **11**, 1018 10.1038/s41419-020-03228-9
44. Struhal, W., Presslauer, S., Spielberger, S., Zimprich, A., Auff, E., Bruecke, T. *et al.* (2014) VPS35 Parkinson's disease phenotype resembles the sporadic disease Journal of Neural Transmission **121**, 755-759 10.1007/s00702-014-1179-1
45. Hinault, M. P., Cuendet, A. F., Mattoo, R. U., Mensi, M., Dietler, G., Lashuel, H. A. *et al.* (2010) Stable alpha-synuclein oligomers strongly inhibit chaperone activity of the Hsp70 system by weak interactions with J-domain co-chaperones J Biol Chem **285**, 38173-38182 10.1074/jbc.M110.127753
46. Zondler, L., Kostka, M., Garidel, P., Heinzelmann, U., Hengerer, B., Mayer, B. *et al.* (2017) Proteasome impairment by alpha-synuclein PLoS One **12**, e0184040 10.1371/journal.pone.0184040
47. Deas, E., Cremades, N., Angelova, P. R., Ludtmann, M. H., Yao, Z., Chen, S. *et al.* (2016) Alpha-Synuclein Oligomers Interact with Metal Ions to Induce Oxidative Stress and Neuronal Death in Parkinson's Disease Antioxid Redox Signal **24**, 376-391 10.1089/ars.2015.6343
48. Shamoto-Nagai, M., Hisaka, S., Naoi, M., andMaruyama, W. (2018) Modification of α-synuclein by lipid peroxidation products derived from polyunsaturated fatty acids promotes toxic oligomerization: its relevance to Parkinson disease Journal of Clinical Biochemistry and Nutrition **62**, 207-212 10.3164/jcbn.18-25
49. Fani, G., La Torre, C. E., Cascella, R., Cecchi, C., Vendruscolo, M., andChiti, F. (2022) Misfolded protein oligomers induce an increase of intracellular Ca(2+) causing an escalation of reactive oxidative species Cell Mol Life Sci **79**, 500 10.1007/s00018-022-04513-w
50. Nakamura, K., Nemani, V. M., Azarbal, F., Skibinski, G., Levy, J. M., Egami, K. *et al.* (2011) Direct membrane association drives mitochondrial fission by the Parkinson disease-associated protein alpha-synuclein J Biol Chem **286**, 20710-20726 10.1074/jbc.M110.213538
51. Nakamura, K., Nemani, V. M., Wallender, E. K., Kaehlcke, K., Ott, M., andEdwards, R. H. (2008) Optical reporters for the conformation of alpha-synuclein reveal a specific interaction with mitochondria J Neurosci **28**, 12305-12317 10.1523/JNEUROSCI.3088-08.2008
52. Tang, F. L., Liu, W., Hu, J. X., Erion, J. R., Ye, J., Mei, L. *et al.* (2015) VPS35 Deficiency or Mutation Causes Dopaminergic Neuronal Loss by Impairing Mitochondrial Fusion and Function Cell Rep **12**, 1631-1643 10.1016/j.celrep.2015.08.001